ARTICLES

A 150,000-year climatic record from Antarctic ice

C. Lorius*, J. Jouzel[†], C. Ritz*, L. Merlivat[†], N. I. Barkov[‡], Y. S. Korotkevich[†] & V. M. Kotlyakov[§]

* Laboratoire de Glaciologie et de Géophysique de l'Environnement, CNRS, BP96, 38402 Saint Martin d'Héres Cedex, France
† Laboratoire de Géochimie Isotopique DPC, CEN Saclay, 91191 Gif-sur-Yvette Cedex, France
‡ The Arctic and Antarctic Research Institute, Fontanka 34, Leningrad 191104, USSR
§ Institute of Geography, Academy of Sciences of USSR, Staronometry, St 29, Moscow 109017, USSR

During much of the Quaternary, the Earth's climate has undergone drastic changes most notably successive glacial and interglacial episodes. The past 150 kyr includes such a climatic cycle: the last interglacial, the last glacial and the present holocene interglacial. A new climatic-time series for this period has been obtained using $\delta^{18}O$ data from an Antarctic ice core.

ALTHOUGH continuous records of climatic and environmental conditions extending beyond 150 kyr are preserved in polar ice sheets, a reliable time series covering the whole of this climatic cycle has not yet been derived from ice cores. This results from logistic reasons, the favourable sites being located in the central regions of Antarctica and Greenland, and the technical difficulty of deep drilling.

The Quaternary has undergone successive glacial and interglacial episodes[1-3]. Since the first Camp Century drilling in north-west Greenland[4], five deep-ice cores reaching back to the last glacial have been recovered in Antarctica at Byrd[5], Vostok[6] and Dome C[7] and in Greenland at Dye 3[8]. They have been extensively studied for their oxygen-18 content (denoted $\delta^{18}O$ expressed with respect to SMOW) and their chemical impurities, which provide valuable information about the Earth's palaeoclimate and palaeoenvironment (see refs 9, 10).

Of these cores, Camp Century seems to extend back to the last interglacial. As it was drilled down to the bedrock, however, this last interglacial ice is confined to the last few metres of the core, because of the thinning of the ice layers during their sinking in the ice sheets. The complexity of the flow lines makes it difficult to date ice cores reaching the bedrock by flow modelling only. Indirect dating techniques, based on the comparison of $\delta^{18}O$ profiles in ice cores and in deep-sea cores have recently been used[7-9] for this purpose. A new Camp Century timescale was proposed which confirms the presence of last interglacial ice and, accordingly, indicates that the deepest part of the Dye 3 ice core was probably deposited during this period[9]. This is possibly also the case for the Devon Island core drilled through a shallow ice cap in the Canadian Arctic[11].

We have determined a new climatic-time series obtained from $\delta^{18}O$ analysis of a 2,083-m ice core drilled at Vostok Station by the Soviet Antarctic Expeditions. The site is located on the high Antarctic Plateau, where the ice thickness is ~3,700 m. The isotope profile covers the last 150 kyr, back to the ice age which preceeded the last interglacial, and has essentially been undisturbed by flow conditions.

Vostok ice core

The Soviet Antarctic station of Vostok is located in East Antarctica (78°28' S and 106°48' E) at an altitude of 3,488 m (mean annual pressure 624 mbar; mean annual temperature −55.5°C). The present snow accumulation is between 2.2 and 2.5 g cm^{-2} yr$^-$ (ref. 12) as determined independently from a profile of artificial β activity[13] and detailed stake measurements[14].

The first series of drilling was performed down to 950 m in successive steps between 1970 and 1974. This 950-m core covers all the Holocene and part of the last glacial periods as shown by the $\delta^{18}O$ profiles obtained by Barkov and co-workers[6,15,16]. In 1980, the drilling of a second deep hole was started which

has reached a depth of 2,083 m. The $\delta^{18}O$ measurements were completed down to 1,412 m (refs 17, 18), a depth which would correspond, from a preliminary dating, to 115 kyr BP (ref. 19).

The collaboration between Soviet and French scientists which centred around the study of this new 2,083-m Vostok ice core was initiated in 1982. Within this framework, sampling was done in the field during the 1982-83 Austral summer and pieces of ice core were sent to Grenoble. The core analysis now in progress in various Soviet and French laboratories concerns, in particular, the chemical analysis of impurities and gas bubbles including CO_2.

$\delta^{18}O$ profile

Sampling of ice for isotope analysis was done in the field (1982-83 Austral summer) by cutting a continuous slice from the length of the ice after careful cleaning. Sampling was performed on 1.5-2 m ice increments. Samples were sent in solid form to Grenoble and then melted before isotope analysis in Saclay. Two independent series of samples were obtained: (1) a discontinuous series, duplicated to check reproducibility, with one sample taken each 25 m from the surface down to the bottom of the core; (2) a continuous series between 1,406 and 2,083 m.

Oxygen-18 and deuterium determinations were simultaneously performed on all the samples. Here we will discuss the $\delta^{18}O$ results. The deuterium and deuterium-excess[20] results will be discussed elsewhere. The results, obtained with an accuracy of ±0.15‰ (w.r.t. SMOW), are shown in Fig. 1 as a function of the sample depth. The two sets of samples from the discontinuous series are in good agreement all along the core and their average value at each level is given. For the sake of discussion a continuous line was drawn between each point. There is excellent agreement between the continuous and discontinuous series over all the common parts indicating that the 25-m sampling interval is fine enough to extract reliable palaeoclimatic information. On the other hand, the present data are not detailed enough to document for the Southern Hemisphere such features as the abrupt environmental changes revealed in the Dye 3 ice core between 30 and 40 kyr BP (refs 9, 21).

Down to 1,400 m, the basic features of the $\delta^{18}O$ curve (Fig. 1) are similar to previously published Vostok $\delta^{18}O$ profiles[17,18], with the last glacial maximum around 400 m, and a $\delta^{18}O$ shift between glacial and post-glacial conditions of ~5‰. However, there is a systematic shift towards lower values for the present set of data of ~3‰. Such a shift has already been noticed by Dansgaard et al.[22].

The $\delta^{18}O$ profile presented here gives a complete picture of the last climatic cycle from the end of the previous glaciation. In particular, the last interglacial with the highest $\delta^{18}O$ values around 1,825 m can now be examined in detail. For a further
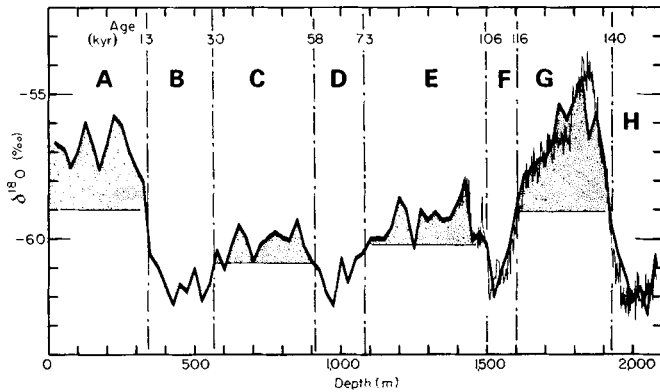
Fig. 1 Oxygen-18 versus depth in the Vostok ice with the definition of the successive stages and indication of the ages corresponding to the limits between these stages. The thick line is drawn from discontinuous data (one for each 25 m), the thin line corresponds to a continuous sampling between 1,400 and 2,083 m. For explanation of A-H, see text.
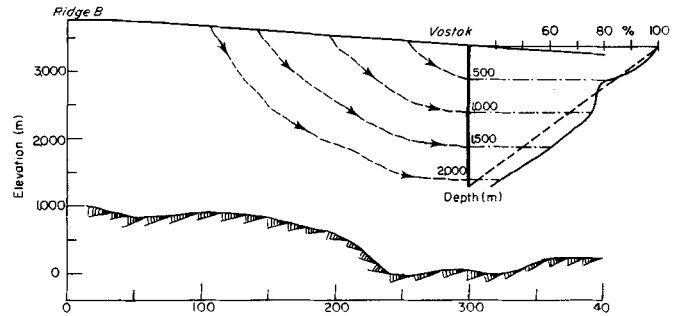

Fig. 2 Surface and bedrock topography along the Ridge B-Vostok axis (lower curve) and the thinning function (top right) expressed as a percentage of the initial thickness, with (solid line) or without (dotted line) taking into account this topography.

description of this curve and comparison with other palaeoclimatic profiles, we will designate the successive warm and cold stages consecutively from the top of the record downwards. A striking feature of the profile is the existence of four very well-marked cold periods (that is, low $\delta^{18}O$) around 425, 975, 1,525 and 2,050 m with practically the same $\delta^{18}O$ values of around −62‰. This makes the definition of the successive stages shown on Fig. 1 relatively straightforward. Starting from the top, the warm periods (hatched areas), are designated by A, C, E and G and the cold periods by B, D, F and H. Stages A and G have the isotopically richest values lying around −57 and −55‰, respectively. From the solid curve (Fig. 1), one can note a sharp isotope transition (~2‰) inside the G stage at a depth of 1,790 m. Stages E and C are relatively warm interstadials intermediate between full glacial and interglacial conditions.

Dates for the limits between the successive phases are indicated on the top of Fig. 1 (the dating method used is described below). Stage A corresponds to the present Holocene period. Stages B-F cover the last glacial. Stage G includes the peak of the last interglacial and stage H is the last part of the previous glacial.

Ice-core chronology

Many techniques, including isotope and chemical stratigraphies and flow modelling, have been used over the past 10 yr to establish dating of the Vostok ice[16,19,23,24]. Further detailed isotope study showed that seasonal $\delta^{18}O$ variations are rapidly smoothed by diffusion[22] indicating that reliable dating cannot be obtained from isotope stratigraphy. Unlike the Camp Century core, where the existence of interglacial ice relies on a comparison with deep-sea core isotope profiles, we propose to establish the timescale using an ice-flow model which is independent of other palaeoindicators.

There are two problems with this type of dating. First, for each depth the rate of accumulation at the time and in that area of origin of snow, $A(z)$, must be determined. Second, the thinning function, that is, the ratio of the thickness of a layer to its initial thickness, has to be calculated. We now describe our approach to these problems.

To estimate the past accumulation rate we adopt a procedure based on the observation that the present precipitation rate on the Antarctic plateau is strongly correlated with suface temperature. Robin[25] has suggested that this correlation exists because precipitation is governed by the amount of water vapour in the atmosphere circulating above the surface inversion layer. As discussed by Lorius et al.[7] and Jouzel and Merlivat[26], there is a link between the temperature of formation of precipitation and its oxygen isotope ratio. Assuming that the same relationship has held in the past, it is thus possible to estimate past accumulation rates from the $\delta^{18}O$ profile of the ice. Raisbeck et al.[27] and

Yiou et al.[28] in this issue have noted that the ^{10}Be concentrations of ice at Dome C and Vostok are consistent with accumulation rates deduced by such procedures. We thus estimate the accumulation function in the following way. First, the temperature of formation of precipitation, T_F, is estimated along the profile as described by Lorius et al.[10]. Then, the accumulation rate, $A(z)$, is calculated from the product of its present value, $A(0)$, times the ratio of the derivatives of the saturation vapour pressure— with respect to $T_F(z)$ for the time of precipitation and with respect to $T_F(0)$ for the present conditions. This formulation is derived from a simplified unidimensional model neglecting the possible changes in circulation intensity above the area of precipitation.

The use of a two-dimensional glaciological model is well suited to the Vostok area as the ice flowlines are roughly parallel in this region of East Antarctica[29]. The change of the ice thickness upstream of the drilling site is important because of the bedrock topography[30] (Fig. 2) and this has been taken into account when using the analytical model of Lliboutry[31]. Finally, ice-core dating is established using an iterative process. Starting from a plausible dating obtained from a simple one-dimensional model the ice origin is determined. Then, the thinning function is calculated and the ice redated all along the core. The process is repeated using the new dates as the initial conditions until the initial and final datings converge.

To illustrate the influence of the bedrock topography, the thinning functions with (Fig. 2, solid line) and without (Fig. 2, dotted line) taking into account this topography can be compared. This demonstrates the strong effect of bedrock topography between 500 and 1,000 m. For these calculations, ice velocities were approximated by their average values using mass continuity over the entire climatic cycle.

The results are presented in Fig. 3 for three values of the present accumulation. The annual accumulation (expressed with respect to its present value) is obviously correlated to the $\delta^{18}O$ profile with lower values during glacial periods as previously stated from Dome C ice-core studies[7,27] and independently proposed at Vostok from ^{10}Be measurements[28].

From available data[12], an average value of 2.3 g cm^{-2} yr^{-1} was adopted for the present accumulation rate, giving ages of 98 kyr BP at 1,412 m (that is, significantly younger than the previously estimated[19] 115 kyr BP) and of ~160 kyr BP for the bottom of the core.

This accumulation value, although uncertain given the very short period (<10 yr) over which this parameter was determined, seems to be a reasonable average over the Holocene period. Our dating puts the end of the last climatic transition at around 10 kyr BP which compares well with the same event recorded in the Dome C East Antarctic core at ~10.5 kyr BP (ref. 7). The uncertainty on this value is thus ~5%, a value which would give a lower limit for the relative dating uncertainty all along the core. Dating of the first part of the core is also indirectly supported by the existence of a dust content maximum between ~13 and 26 kyr BP (ref. 32), a period of aridity over Australia[33].

However, other sources of errors come from estimations of accumulation changes and, to a lesser degree, of the thinning function. Thus, the age of the bottom of the core is probably not known with a precision better than 10–15 kyr.

Palaeoclimatic information

The isotope content of polar snow is primarily governed by T_F, but it also depends[9,10,34,35] on several other parameters such as the origin and dynamical history of the air masses and the microphysical processes leading to snow formation. A way of reconstructing the full, space-time variations of isotope contents of vapour and precipitation is to incorporate the isotope cycles in a general circulation model of the atmosphere (GCM)[36].

Until this new approach is fully developed, the climatic interpretation must be based on $\delta^{18}O$-temperature relationships observed in modern precipitation and/or isotope models which give only a simple schematic overview of the dynamic history of the air masses. Although aware of the limitations, we are relatively confident that when the two methods are combined major temperature changes, such as those accompanying glacial-interglacial transitions, can be estimated. This is especially true for central East Antarctica for several reasons. First, the observed $\delta^{18}O$-temperature relationship[37] is quite linear (correlation coefficient, $r = 0.989$ for the -20 to $-55\,°C$ interval) and its slope can be correctly explained on a theoretical basis applying a recently developed kinetic isotopic model[26]. Second, the ice thickness has probably undergone only minor fluctuations and the ice origin can be reliably reconstructed. In addition, our confidence in a temperature reconstruction is reinforced in the Vostok core by the good agreement between accumulation changes derived by transforming the $\delta^{18}O$ profile into a temperature profile and those derived from [10]Be (ref. 28).

After correcting for the change in $\delta^{18}O$ of the oceanic water (maximum $1.6‰$)[3], this temperature reconstruction is carried out as in ref. 10. With this interpretation, the glacial-interglacial surface temperature shifts are $\sim 10\,°C$ for the H–G transition ($\delta^{18}O$ shift of $6.5‰$) and $8\,°C$ for the B–A transition ($\delta^{18}O$ shift of $5‰$). C and E interstadials are around 2 and 4 $°C$, respectively, warmer than full glacial conditions and the four cold stadials H, F, D and B are within $\sim 1\,°C$. The peak of the last interglacial maximum is significantly warmer than the Holocene period. The difference is estimated to $\sim 3\,°C$, $1\,°C$ of this being due to the formation of the interglacial ice 100 km further inland (Fig. 2). All these values do not take into account the possible variations in the ice-cap altitude. These corrections will be done, if necessary, from the total gas content which is under investigation. Preliminary data (D. Raynaud, personal communication) suggest that the isotope signal is essentially of climatic origin which is independently corroborated by some studies tending to demonstrate the relative stability of the East Antarctic ice sheet at the considered timescale[38,39].

Comparison with other ice cores

Concerning the transition between the last glacial maximum (around 18 kyr BP) and the Holocene periods (B–A in our terminology), the present results confirm the excellent agreement between the two East Antarctic sites, with a $\delta^{18}O$ shift, before corrections, of $5.4‰$ at Dome C[7] and of $\sim 5‰$ at Vostok, and to a lesser degree with the Byrd West Antarctic site (shift of $7‰$)[5]. The inferred surface temperature change for Antarctica is ~ 8–$10\,°C$. These shifts agree well with those deduced for high southern latitudes from GCM ice-age modelling[40,41], although recent simulations predict lower temperature shifts[42,43]. The isotope shift is also $7‰$ in southern Greenland (Dye 3)[8,9]. The higher values ($>10‰$) registered in northern Greenland and adjacent regions (Camp Century, Devon Island) can be partly attributed either to a change in the elevation of the ice formation[44] or to a more drastic climatic change in this area than in southern Greenland or in Antarctica[9].

For the last glacial, a detailed comparison with other ice cores is difficult because only 7% of the Vostok core was analysed down to 1,400 m. In any case, it would be necessary to discuss
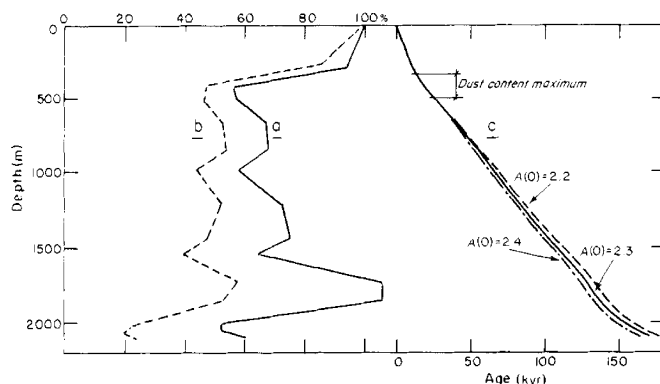
Fig. 3 *a*, Initial thickness of annual layers (accumulation rate $A(z)$); *b*, thickness of these annual layers in the core. Both *a* and *b* are expressed with respect to the present (accumulation rate $A(0)$); *c*, depth-age relationship for different values of $A(0)$ in $g\,cm^{-2}\,yr^{-1}$.

thoroughly the successive timescales derived for the Byrd, Camp Century and Dye 3 cores. Such a comparison will be undertaken in the near future when a continuous profile becomes available for the Vostok core.

The apparent time elapsed between the interglacial peak and the following $\delta^{18}O$ minimum is more than twice as long at Vostok than at Camp Century. This is not strictly an ice core feature and cannot be discussed further here (see below) as the Camp Century timescale is deduced from a comparison with the deep-sea record[9]. This shows the difficulty of applying such an indirect dating method.

Comparison with $\delta^{18}O$ in deep-sea cores

It is now widely accepted that $\delta^{18}O$ in benthic foraminifera primarily reflects ice-volume changes[3,45,46]. Although the relationship can be distorted by many factors, the CLIMAP project members concluded that there is no compelling evidence to reject the first-order assumptions of isotope synchroneity or fidelity to the ice volume[45]. Although varying in detail, all the cores give similar general trends[3,47], allowing a common definition of isotope stratigraphy. The period of interest here covers Emiliani's stages 1–6 (ref. 48), stage 5 being subdivided in 5a to 5e (ref. 49), as we have illustrated on Fig. 4e.

With the adopted Vostok dating, there is a good correspondence between stages 1–4 and Vostok stages A–D. Stage E covers 5a–5c and F corresponds to 5d. However, there is no clear correspondence between 5e and G representing the last interglacial in deep-sea and ice records, respectively (Fig. 4). There is a major difference in the duration of these two stages; 11 kyr for 5e and 24 kyr for G. Also, the last interglacial peak in the Vostok core is around 130 kyr BP whereas the corresponding ice-volume minimum in the deep-sea record is dated earlier at 122-kyr BP (ref. 45).

A doubling of the accumulation rate over this period would lead to a good correspondence between the 5e and G stages. While this possibility cannot be completely ruled out, there is no indication of such a drastic change in the precipitation regime. Part of the time-lag between the two peaks could be real (~ 3 kyr) as already observed between Southern Hemisphere ocean temperature and ice volume records but dating uncertainties (probably of ~ 10 kyr at this level) prevent a detailed discussion of this possible lag. On the other hand, the fact that ice stage G probably lasted longer than stage 5e is a key element for understanding the last interglacial climate and the initiation of the last ice age. A detailed interpretation is beyond the scope of the present study and would require knowledge of the exact timing between the temperature and ice volume signals. Recent measurements of $\delta^{18}O$ of air entrapped in ice cores could provide a way of correlating deep-sea and ice-cores $\delta^{18}O$ profiles and then establishing this timing[50].

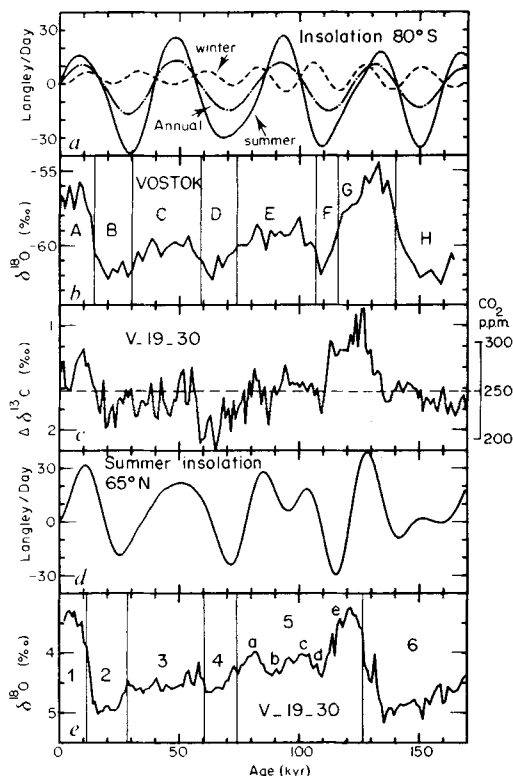**Fig. 4** Variation with time of: a, winter, summer and annual insolations at 80° S (ref. 59); b, $\delta^{18}O$ in the Vostok ice (this work); c, $\Delta\delta^{13}C$ in the V 19-30 deep-sea core[68] and indication of the CO_2 scale on the right; d, summer insolation at 65° N (ref. 59); e, $\delta^{18}O$ in the V 19-30 deep-sea core[68] for Uvigerina Senticosa with an indication of the successive climatic stages.

According to CLIMAP members[45], the last interglacial was similar to the current climate. However, they noted some indications of a slightly warmer climate. The Vostok record brings quantifiable evidence of atmospheric warming over Antarctica during this period. This is useful information because there is some controversy about the behaviour of the East Antarctic ice sheet during the last interglacial[45]. In addition, the Vostok record does not support an interglacial character for marine stage 5c (first part of E), an argument used to suggest an East Antarctic ice surge around 95 kyr BP (ref. 51).

Whereas glacial buildups in the deep-sea record (Fig. 4e) are gradual·giving the ice-volume cycles their asymmetrical saw-toothed character[52], the ice record (Fig. 4b) shows that the minimum temperatures were of the same order during cold periods (H, F, D and B stages). This may be linked to the rapid response of the atmospheric system to forcings and feedbacks and also suggests that there is a very stable mode of the climatic system for these cold periods. Such differences in shape were previously noted between ice-volume and temperature signals recorded in some oceanic cores[53].

Forcing and feedback factors

Beyond this reconstruction of the East Antarctic climate, we now discuss some current important aspects of the mechanisms which have probably controlled this climate and how the East Antarctic climate is related to the global climate. We will examine the possible role of changes in insolation, atmospheric CO_2 content and global ice volume.

Insolation changes. Over recent years, the Milankovitch hypothesis that orbital variations are the principal causes of the Pleistocene ice ages has received considerable support[45,52-54], and has stimulated many modelling efforts[55-58]. The spectral analysis of proxy records has revealed periodicities statistically correlated to the precessional (19 and 23 kyr), obliquity (41 kyr) and eccentricity (100 kyr) cycles. There is a general consensus

that summer insolation at about 65° N might be a plausible forcing as Northern Hemisphere ice sheets have undergone the major changes, and that the dominant 100-kyr cycle would result from a nonlinear response of ice sheets to orbital forcing.

Before discussing the possible link between the Northern Hemisphere insolation changes and the Vostok climate, we will investigate whether there is a relationship between this climate and the local changes of insolation.

The comparison of the $\delta^{18}O$ ice profile (Fig. 4b) with the annual insolation curve for 80° S (ref. 59) (Fig. 4a) reveals a very striking relationship between the cold and warm isotope stages and the minima and maxima of the insolation curve. While discontinuous sampling prevents us from performing reliable spectral analysis, especially for short periodicities, this remarkable correlation strongly supports the role of orbital forcing in climatic change.

The particular importance of the obliquity cycle, previously suggested from some high-latitude oceanic cores[54], would indicate that orbital forcing acts at a local scale. At 80° S, the maximum change of annual insolation is ~7% (ref. 59) which, from the radiative equilibrium equation, corresponds to a direct temperature effect of 4 °C. This direct effect is certainly important when compared with the 10 °C temperature range inferred from the $\delta^{18}O$ profile.

The apparent climatic synchroneity between the Northern and Southern Hemispheres poses a problem because the seasonality history of the polar insolation at 65° is different for the two hemispheres[60,61]. One explanation[61] could be that, for polar regions, the climate responds to annnual insolation changes that are in phase for the two hemispheres. The correlation between the 80° S annual insolation and the $\delta^{18}O$ record gives some support to this hypothesis.

Finally, accepting the role of orbital forcing on the Southern Hemisphere climate, the existence of a roughly 40-kyr cycle in the $\delta^{18}O$ ice core record indirectly supports the Vostok core dating.

Atmospheric CO_2 concentration. CO_2 measurements from the analysis of air bubbles entrapped in ice from Greenland and Antarctic cores have shown that CO_2 changes are associated with climatic changes. Such direct measurements are available for the past 40 kyr (refs 62-65) and show a CO_2 increase of ~40% between the last glacial maximum and the pre-industrial Holocene period. These measurements suggest that CO_2 and its greenhouse warming might be involved in the control of the ice ages[21] and also in their interhemispheric synchroneity[42,60].

Shackleton et al.[66] have used the idea that the difference in carbon isotope ratios in surface and deep oceanic waters varies with CO_2 levels[67] to develop an indirect approach which extends the atmospheric CO_2 record further back in time. They estimate this parameter from the $\delta^{13}C$ difference between planktonic and benthic foraminifera ($\Delta\delta^{13}C$). The validity of this approach is supported by the fact that the estimated CO_2 values are consistent with the polar record over their common part[66] (the past 40 kyr). However, because many assumptions underly this method, it has to be corroborated either from other oceanic cores or, more directly, from ice cores. A study is in progress to obtain a detailed CO_2 profile along the Vostok core to examine directly the CO_2-climate connection over the past 150 kyr. In the following discussion, we will treat the $\Delta\delta^{13}C$ curve as a CO_2 curve.

The first 150 kyr of this $\Delta\delta^{13}C$ record[68] is shown on Fig. 4c. One can easily see the similarities between this curve and the $\delta^{18}O$ Vostok record. A relationship between CO_2 content and atmospheric temperatures is expected. Indeed, climate models predict that the greenhouse CO_2 effect should be amplified in high latitudes especially near ice margins[69,70]. Thus, these observed similarities suggest a CO_2-atmospheric temperature connection all over the last climatic cycle. According to Stauffer et al.[21] a 40-% CO_2 change corresponds to a temperature rise of 2-4.5 °C in high latitudes. Thus, the hypothesis that CO_2 changes are an important factor in controlling high latitude climate is well within the realm of possibility.

There are several other features of the CO_2–climate relationship. CO_2 measurements at Dome C indicate that the increase in CO_2 concentration associated with the end of the last ice age began before, or simultaneously with, the climatic change at high southern latitudes[65]. On the other hand, from the 340-kyr reconstructed CO_2 curve, Pisias and Shackleton[71] inferred that CO_2 lags the orbitals forcing (summer insolation at 65° N) but leads the ice volume, by an average of 2.5 kyr. From this, they made two important points[68,71]: (1) CO_2 changes are not a consequence of climatic changes but may represent part of the mechanisms by which orbital variations induce changes in climate; (2) the presence of a strong obliquity component suggests a high-latitude control for the mechanisms by which CO_2 responds to orbital forcing.

This also puts constraints on the way in which CO_2 levels in the ocean surface, which eventually control the atmospheric CO_2 levels, can vary[68]. Recently, four groups[72-75] have independently explored CO_2 scenarios implying a high latitude control through: the changes in ocean circulation; the influence of the amount of light reaching the polar regions on the utilization of nutrients; and a combination of these two factors.

The Knox and McElroy nutrient scenario[74] includes a mechanism whereby small changes in insolation at high latitudes could result in large changes in CO_2 and thus looks attractive in view of the possible CO_2 climatic role at the timescale considered here although this type of scenario[78] is not supported by recent results on planktonic foraminifera from Antarctic deep-sea sediments.

Ice-volume feedbacks. Although many assumptions are involved, the above discussion suggests that local insolation and possibly the atmospheric CO_2 have played a part in determining the Antarctic climate over the past 150 kyr. The two factors alone, however, would not explain all the climatic variability seen in the $\delta^{18}O$ Vostok record. In particular, we observe that the very cold stage F corresponds to an intermediate inferred CO_2 value.

Note that this stage F corresponds to the time of lowest insolation at 65° N (Fig. 4d)[59]. (Indeed, there are similarities between this insolation curve and the $\delta^{18}O$ Vostok record (Fig. 4b) over all the past 150 kyr.) Modelling of the growth and retreat of the ice sheets has shown that ice volume changes can be driven by summer radiation in Northern Hemisphere high latitudes[56,57,76,77]. Although all of the models do not specifically refer to 65° N, the generated ice-volume curves resemble, with a few kiloyears lag, the summer insolation at this latitudinal band. As shown in Fig. 4d, high volumes correspond to low insolations and vice versa. Such generated ice volume curves differ from ice volumes deduced from benthic foraminifera (Fig. 4e). In particular, note the difference during stage F. According to Budd[61] the two approaches of deriving ice volumes can be reconciled if the contribution of ^{18}O-poor Antarctic ice is taken into account. This raises the question of how Northern Hemisphere ice extent can influence Antarctic climate.

Although we cannot answer this question here, we note that recent GCM results[42] show that such a relationship cannot be explained by the interhemispheric exchange of heat in the atmosphere. Other mechanisms would have to be involved, such as a change in the cross-equatorial heat transport by the ocean circulation[42,60,78] or a response of the East Antarctic ice sheets to sea-level changes[61]. This second hypothesis is valid only if its apparent contradiction with the time lead of Antarctic sea-ice compared with the Northern Hemisphere ice volume can be solved as suggested by Budd[61].

Conclusions

We have obtained the first complete and unambiguous isotope description from a deep-ice core of the last climatic cycle. The 2,083-m Vostok record covers the past 150 kyr extending into the end of the previous glacial period. The timescale has been established by combining a glaciological model appropriate here as the core represents only about the first half of the ice sheet, with an original approach for estimating past accumulation rates from the isotope record. While this method has its own limita-

tions, it has the advantage of being independent of other palaeo-indicators or climatic forcing series.

This $\delta^{18}O$ record has been interpreted as essentially representing temperature changes over East Antarctica. This interpretation is based on the $\delta^{18}O$–temperature gradient observed for modern precipitation and on a dynamically-simple isotope model. Although aware of the necessity of a more detailed modelling of the atmospheric $\delta^{18}O$ cycle using GCMs, we have confidence in the temperature interpretation as far as major $\delta^{18}O$ changes are concerned.

In this interpretation, the Vostok record provides extremely rich climatic information. The present Holocene period was preceded by a long glacial period marked by two relatively warm interstadials. The well-marked last interglacial was significantly warmer than the Holocene and the end of the previous glacial was quite similar to the last glacial maximum.

A comparison with $\delta^{18}O$ in deep-sea cores shows that the Antarctic climate and the global ice volume have not evolved in the same way. The last interglacial appears to be about twice as long in the Antarctic temperature record as in the ice-volume record. In addition, there are marked differences in the shapes of the records during the last glacial. Thus, we now have access to another different, but complementary, climatic record fully covering the last climatic cycle.

The presence of a roughly 40-kyr cycle in the Vostok record strongly supports the role of orbital forcing in determining climatic changes. This record is approximately in phase with the annual insolation at 80° S suggesting that this forcing operates at a local scale. There are also some common features between the climatic curve and the summer insolation at 65° N which may be the result of the influence of the Northern Hemisphere ice sheets on the Antarctic climate.

There are striking similarities between the $\Delta\delta^{13}C$ curve of Shackleton and co-workers[66,68] and the $\delta^{18}O$ record. Following these authors in treating the $\Delta\delta^{13}C$ curve as a CO_2 curve, there appears to be, over a complete climatic cycle, a relationship between atmospheric CO_2 levels and atmospheric temperatures as previously suggested for the past 40 kyr.

There are several other ways to obtain more climatic information from the Vostok ice than the $\delta^{18}O$ method described here. Interesting results concerning ^{10}Be have been obtained[27], and other studies are either in progress or planned for the near future. They include additional deuterium and oxygen-18 determinations and measurements of total gas volume, crystal size, CO_2 in the air bubbles, $^{18}O/^{16}O$ ratio of oxygen in air and aerosol content.

The Vostok ice core offers the possibility of measuring many other parameters and their variation with time. As shown from other ice cores, the number of these parameters of interest is growing. Recent studies include more and more chemical elements[79-83] and trace gases[84] as well as $^{12}C/^{13}C$ ratio in CO_2 (ref. 85). Although their first objective is to reconstruct the Earth's palaeo-environment, some of these parameters also contain, at least indirectly, palaeoclimatic information. Finally, it is hoped to reach greater depths in the Vostok drilling and thus to extend the time scale considerably.

1. Shackleton, N. J. Nature 215, 15–17 (1967).
2. Shackleton, J. J. & Opdyke, N. D. Quat. Res. 3, 39–55 (1973).

3. Duplessy, J. C. *Climatic Change* (ed. Gribbin, J.) 46–67 (Cambridge University Press, 1978).
4. Dansgaard, W., Johnsen, S. J. Moeller, J. & Langway, C. C. *Science* 166, 377–381 (1969).
5. Epstein, S., Sharp, R. P. & Gow, A. J. *Science* 168, 1570–1572 (1970).
6. Barkov, N. I., Korotkevitch, E. S., Gordienko, F. G. & Kotlyakov, V. M. *IAHS Publ.* 118, 312–321 (1977).
7. Lorius, C., Merlivat, L., Jouzel, J. & Pourchet, M. *Nature* 280, 644–648 (1979).
8. Dansgaard, W. *et al. Science* 218, 1273–1277 (1982).
9. Dansgaard, W. *et al. Geophys. Monogr.* (M. Ewing Symp., 5) 29, 288–298 (1984).
10. Lorius, C., Raynaud, D., Petit, J. R., Jouzel, J. & Merlivat, L. *Annls Glaciol.* 5, 88–94 (1984).
11. Paterson, N. S. B. *Nature* 266, 508–511 (1977).
12. Young, N. W., Pourchet, M., Kotlyakov, V. M., Korolev, P. A., & Dyugerov, M. B. *Annls Glaciol.* 3, 333–338 (1982).
13. Lorius, C. *et al. IAHS Publ.* 86, 3–15 (1970).
14. Barkov, N. I. *Antarct. J. U.S.* 10, 55–56 (1975).
15. Barkov, N. I., Gordienko, F. G., Korotkevich, E. S. & Kotlyakov, V. N. *Dokl. Acad. Sci. USSR* 214, 1383–1386 (1974).
16. Barkov, N. I., Gordienko, F. G., Korotkevich, E. S. & Kotlyakov, V. M. *Inform. Bull. Soviet Antarct. Expedn.* 90, 39–48 (1975).
17. Gordienko, F. G., Kotlyakov, V. M., Barkov, N. I., Korotkevich, T. E. & Nikolaev, S. D. *Data Glacio* Stud. Acad. Sci. USSR 46, 168–171 (1983).
18. Grosvald, M. G. *Data Glaciol. Stud. Acad. Sci. USSR* 46, 171–174 (1983).
19. Shumskii, P. A., Korotkevich, E. S. & Larina, T. B. *Inform. Bull. Soviet Antarct. Expedn.* 100, 41–48 (1980).
20. Jouzel, J., Merlivat, L. & Lorius, C. *Nature* 289, 688–691 (1982).
21. Stauffer, B., Hofer, H., Oeschger, H., Schwander, J., & Siegenthaler, U. *Annls Glaciol.* 5, 160–164 (1984).
22. Dansgaard, W., Barkov, N. I. & Splettstoesser, J. *IAHS Publ.* 118, 204–209 (1977).
23. Wilson, A. T. & Hendy, C. H. *J. Glaciol.* 27, 95, 3–9 (1981).
24. Budd, W. F. & Young, N. W. *The Climatic Record in Polar Ice Sheets* (ed. de Q. Robin, G. 150–176 (Cambridge University Press, 1983).
25. Robin, G. de Q. *Philos. Trans. R. Soc.* B280, 143–148 (1977).
26. Jouzel, J. & Merlivat, L., *J. geophys. Res.* 89, 11749–11758 (1984).
27. Raisbeck, G. M. *et al. Nature* 292, 825–826 (1981).
28. Yiou, F., Raisbeck, G. M., Bourles, D., Lorius, C. & Barkov, N. I. *Nature* (this issue).
29. Drewry, D. J. *Pol. Rec.* 17, 359–374 (1975).
30. Drewry, D. J. *Scott Polar Research Institute Rep.* (ed. Drewry, D. J.) (Scott Polar Research Institute, Cambridge, 1983).
31. Lliboutry, L. Z. *Gletscherk. Glaziolgeol.* 15, 135–148 (1979).
32. de Angelis, M. *et al. J. atmos. Chem.* 1, 215–239 (1984).
33. Bowler, J. M., *Earth. Sci. Rev.* 12, 279–310 (1976).
34. Robin, G. de Q. *The Climatic Record in Polar Ice Sheets*, (ed. de Q. Robin G.) 180–189 (Cambridge University Press, 1983).
35. Jouzel, J., Merlivat, L., Petit, J. R. & Lorius, C. *J. geophys. Res.* 88, 2693–2703 (1983).
36. Joussaume, S., Jouzel, J. & Sadourny, R. *Nature* 311, 24–29 (1984).
37. Lorius, C. & Merlivat, L. *IAHS Publ.* 118, 127–137 (1977).
38. Alley, R. B. & Whillans, I. M. *J. geophys. Res.* 89, 6487–6493.
39. Drewry, D. J. *Nature* 287, 214–216 (1980).
40. Gates, W. L. *Science* 191, 1138–1144 (1976).
41. Manabe, S. & Hahn, D. G. *J. geophys. Res.* 82, 3889–3911 (1977).
42. Manabe, S. & Broccoli, A. J. *Annls Glaciol.* 5, 100–105 (1984).
43. Hansen, J. *et al. Geophys. Monogr.* 29, 130–163 (1984).
44. Raynaud, D. & Lorius, C. *IAHS Publ.* 118, 326–335 (1977).
45. CLIMAP Project Members *Quat. Res.* 21, 123–224 (1984).
46. Mix, A. C. & Ruddiman, W. F. *Quat. Res.* 21, 1–20 (1984).
47. Imbrie, J. *et al. Milankovitch and Climate* Vol. 1, (eds Berger A. L. *et al.*) 269–305 (Reidel, Dordrecht, 1984).
48. Emiliani, C. *J. Geol.* 63, 538–578 (1965).
49. Shackleton, N. J. *Proc. R. Soc.* B174, 135–154 (1969).
50. Bender, M., Labeyrie, L., Raynaud, D. & Lorius, C. *EOS*, 64, 973 (1984).
51. Hollin, J. T., Nature, 283, 629–633.
52. Broecker, W. S. & Van Donk, J. *Rev. Geophys. Space Phys.* 8, 169–198 (1970).
53. Hays, J. D., Imbrie, J. & Shackleton, N. J. *Science* 194, 1121–1132 (1976).
54. Ruddiman, W. F. & McIntyre, A. *Science* 212, 617–627 (1981).
55. Imbrie, J. & Imbrie, Z. *Science* 207, 943–953 (1980).
56. Budd, W. F. & Smith, I. N. *IAHS Publ.* 131, 369–409 (1981).
57. Pollard, D. *Nature* 296, 334–338 (1981).
58. Le Treut, H. & Ghil, M. *J. geophys. Res.* 88, 5167–5190 (1983).
59. Berger, A. Contr. 37 (Université Catholique de Louvain, Belgique, 1978).
60. Broecker, W. S. *Milankovitch and Climate* Vol. 2 (eds Berger, A. L. *et al.*) 687–698 (Reidel, Dordrecht, 1984).
61. Budd, W. F. *IAHS Publ.* 131, 441–471 (1981).
62. Delmas, R. J., Ascensio, J. M. & Legrand, M. *Nature* 284, 155–157 (1980).
63. Neftel, A., Oeschger, H., Schwander, R. J., Stauffer, B., & Zumbrunn, R. *Nature* 295, 220–223 (1982).
64. Stauffer, B., Hofer, H., Oeschger, H., Schwander, J. & Siegenthaler, U. *Annls Glaciol.* 5, 160–164 (1984).
65. Raynaud, D. & Barnola, J. M. *Annls Glaciol.* 5, 224 (1984).
66. Shackleton, N. J., Hall, M. A., Line, J. & Cang Shuxi *Nature* 306, 319–323 (1983).
67. Broecker, W. S. *Progr. Oceanogr.* 11, 151–197 (1982).
68. Shackleton, N. J. & Pisias, N. G. *Chapman Conf. on* CO_2 (American Geophysical Union, in the press).
69. Manabe, S. & Wetherald, R. T. *J. atmos. Sci.* 37, 99–118 (1980).
70. Washington, W. M. & Meehl, A. G. *J. geophys. Res.* 89, 9475–9503 (1984).
71. Pisias, N. G. & Shackleton, N. J. *Nature* 30, 757–759 (1984).
72. Sarmiento, J. L. & Toggweiller, J. R. *Nature* 308, 621–624 (1984).
73. Siegenthaler, U. & Wenk, T. *Nature* 308, 624–626 (1984).
74. Knox, F. & McElroy, M. B. *J. geophys. Res.* 89, 4629–2637 (1984).
75. Broecker, W. S. & Takahashi, T. *Geophys. Monogr.* (M. Ewing *Symp.*, 5) 29, 314–326 (1984).
76. Birchfield, G. E., Weertman, J. & Lunde, A. T. *Quat. Res.*, 15, 126–142 (1981).
77. Oerlemans, J. *Nature* 297, 550–553 (1982).
78. Broecker, W. S., Peteet, D. & Rind, D. *Nature* 315, 21–26 (1985).
79. Zeller, J. E. & Parker, B. C. *Geophys. Res. Lett.* 8, 895–898 (1981).
80. Legrand, M. & Delmas, R. J. *Atmos Envir.* 18, 1867–1874 (1984).
81. Palais, J. & Legrand, M. *J. geophys. Res.* 90, 1143–1154 (1985).
82. Neftel, A., Jacob, P. & Klockow, D. *Nature* 311, 43–45 (1984).
83. Wolff, E. W. & Peel, D. A. *Nature* 313, 535–540 (1985).
84. Rasmunssen, R. A. & Khalil, M. A. *J. geophys. Res.* 89, 11599–11605 (1984).
85. Friedl, I. H., Moor, E., Oeschger, H., Siegenthaler, U. & Stauffer, B. *Geophys. Res. Lett.* 11, 1145–1148 (1984).

A phage repressor–operator complex at 7 Å resolution

John E. Anderson, Mark Ptashne & Stephen C. Harrison

Department of Biochemistry and Molecular Biology, Harvard University, 7 Divinity Avenue, Cambridge, Massachusetts 02138, USA

The crystal structure of a complex between the DNA-binding domain of phage 434 repressor and a synthetic 434 operator shows that the protein, very similar in conformation to λ repressor, binds to B-form DNA with the second α-helix of a helix–turn–helix motif lying in the major groove.

WE present the X-ray crystal structure at 7 Å resolution of a repressor protein bound to its operator DNA. The protein (also a positive regulator of gene expression) is the amino-terminal, DNA-binding domain of the repressor encoded by coliphage 434, a close relative of phage λ. The operator is a 14-base-pair (bp) synthetic oligonucleotide with 2-fold symmetry that is specifically recognized by 434 repressor. Determination of the structure was facilitated by the preparation of isomorphous repressor–DNA crystals using operator DNA with 5-bromodeoxyuridine instead of thymine at two symmetry-related positions. Important aspects of the structure include: (1) The repressor conformation, predominantly α-helical, is remarkably similar to that of the first four α-helices of λ repressor[1]. (2) The DNA conformation is B-like, with some deviation at the ends of the operator. (3) Repressor contacts the DNA backbone at several distinct points. Bushman *et al.*[2] elsewhere in this issue present evidence that these are sites of strong interaction between repressor and DNA phosphates. (4) An α-helix (α3) lies in the major groove of the DNA and another α-helix (α2) lies across the groove. The helices α2 and α3 correspond to the helix–turn–helix motif found in the crystal structures of three other DNA-binding proteins[1,3,4] (and postulated to occur in many more, including 434 repressor[5-7]). The mode of binding to DNA is similar to that proposed for those proteins on the basis of model building[1,8-10,22], with the α3 helix disposed so that its residues can make sequence-specific contacts with DNA. Changing these residues in the α3 helix of 434 repressor can change the specificity of the repressor (ref. 11 and accompanying paper[12]).

Structure determination

Crystals of the complex of the 434 repressor DNA-binding domain R1-69 and synthetic 434 operator DNA were prepared as described previously[13]. The space group is I422, with $a = b = 166.4$ Å, $c = 139.4$ Å. Each strand of the synthetic DNA operator had the sequence 5′HO-d(A-C-A-A-T-A-T-A-T-A-T-T-G-T)-OH 3′. Derivative crystals were also prepared, using a similar